VILNIUS UNIVERSITY
CPST SEMICONDUCTOR PHYSICS INSTITUTE

SAULIUS NARGELAS

INVESTIGATION OF CARRIER DYNAMICS IN InN, InGaN, AND GaAsBi BY OPTICAL PUMP-PROBE TECHNIQUES

Summary of doctoral thesis
Physical sciences, Physics (02 P), Semiconductor physics (P 265)

Vilnius, 2012

The research has been carried out in 2008–2012 at the Semiconductor Physics Department of Physics Faculty and Institute of Applied Research, Vilnius University.

Scientific supervisor:

Prof. habil. dr. Kęstutis Jarašiūnas (Vilnius University, Physical Sciences, Physics – 02 P, Semiconductor Physics – P 265).

Council of defense of the doctoral thesis of Physical Sciences at Vilnius University:

Chairman:

Prof. habil. dr. Gintautas Tamulaitis (Vilnius University, Physical Sciences, Physics – 02 P, Semiconductor Physics – P 265).

Members:

Prof. habil. dr. Gintaras Valušis (Vilnius University, Physical Sciences, Physics – 02 P, Semiconductor Physics – P 265).

Prof. dr. Vincas Tamošiūnas (Vilnius University, Physical Sciences, Physics – 02 P, Semiconductor Physics – P 265).

Dr. Gediminas Račiukaitis (CPST Institute of Physics, Physical Sciences, Physics – 02 P, Solid State Physics – P 260).

Prof. habil. dr. Eugenijus Šatkovskis (Vilnius Gediminas Technical University, Physical Sciences, Physics – 02 P, Semiconductor Physics – P 265).

Opponents:

Prof. habil. dr. Edmundas Kuokštis (Vilnius University, Physical Sciences, Physics – 02 P, Semiconductor Physics – P 265).

Prof. habil. dr. Sigitas Tamulevičius (Kaunas University of Technology, Physical Sciences, Physics – 02 P, Solid State Physics – P 260).

The official defense of the doctoral thesis will be held in the public session of the Vilnius university Defense Council of Physical sciences at 13 h on December 14, 2012, in 815 lecture room of Faculty of Physics, Vilnius University, Saulėtekio Ave. 9-III, LT-10222 Vilnius, Lithuania.

The summary of the doctoral thesis has been distributed on November …. , 2012.

The doctoral thesis is available at Vilnius University library and at the library of Center for Physical Sciences and Technology.

VILNIAUS UNIVERSITETAS
FTMC PUSLAIDININKIŲ FIZIKOS INSTITUTAS

SAULIUS NARGELAS

NEPUSIAUSVIRŲJŲ KRŪVININKŲ DINAMIKOS TYRIMAS SUŽADINIMO-ZONDAVIMO METODIKOMIS InN, InGaN, GaAsBi

Daktaro disertacijos santrauka
Fiziniai mokslai, fizika (02 P), puslaidininkių fizika (P 265)

Vilnius, 2012

Disertacija rengta Vilniaus universiteto Fizikos fakulteto Puslaidininkių fizikos katedroje ir Taikomųjų mokslų institute 2008–2012 metais.

Mokslinis vadovas:

Prof. habil. dr. Kęstutis Jarašiūnas (Vilniaus universitetas, fiziniai mokslai, fizika – 02P, puslaidininkių fizika – P265).

Disertacija ginama Vilniaus Universiteto Fizikos mokslų krypties taryboje:

Pirmininkas:

Prof. habil. dr. Gintautas Tamulaitis (Vilniaus Universitetas, fiziniai mokslai, fizika – 02 P, puslaidininkių fizika – P 265).

Nariai:

Prof. habil. dr. Gintaras Valušis (Vilniaus Universitetas, fiziniai mokslai, fizika – 02 P, puslaidininkių fizika – P 265).

Prof. dr. Vincas Tamošiūnas (Vilniaus Universitetas, fiziniai mokslai, fizika – 02 P, puslaidininkių fizika – P 265).

Dr. Gediminas Račiukaitis (FTMC Fizikos Institutas, fiziniai mokslai, fizika – 02 P, kondensuotos medžiagos – P 260).

Prof. habil. dr. Eugenijus Šatkovskis (Vilniaus Gedimino technikos universitetas, fiziniai mokslai, fizika – 02 P, puslaidininkių fizika – P 265).

Oponentai:

Prof. habil. dr. Edmundas Kuokštis (Vilniaus Universitetas, fiziniai mokslai, fizika – 02 P, puslaidininkių fizika – P 265).

Prof. habil. dr. Sigitas Tamulevičius (Kaunas technologijos universitetas, fiziniai mokslai, fizika – 02 P, kondensuotos medžiagos – P 260).

Disertacija bus ginama viešame gynimo tarybos posėdyje 2012 m. gruodžio 14 dieną 13 valandą Vilniaus universiteto Fizikos fakulteto 815 auditorijoje, Saulėtekio al. 9, III rūmai, LT-10222 Vilnius, Lietuva.

Disertacijos santrauka išsiuntinėta 2012 m. lapkričio .... d.

Disertaciją galima peržiūrėti Vilniaus univesiteto ir Fizinių ir technologijos mokslų centro bibliotekose.

Santrauka

Pagrindinis disertacijos tikslas – ištirti nepusiausvirųjų krūvininkų dinamikos ypatumus perspektyviose puslaidininkinei elektronikai ir optoelektronikai naujose medžiagose su technologiniškai varijuojamomis savybėmis: InN, InGaN, GaAsBi heterosandarose. Eksperimentinių tyrimų ir jų skaitmeninės analizės keliu įvertinti krūvininkų rekombinacijos ir difuzijos procesų ypatumus bei nustatyti jų parametrus plačiame nepusiausvirųjų krūvininkų tankių (10^{18}–10^{20} cm^{-3}) ir bandinio temperatūrų (10–300 K) intervale, siekiant surasti šių medžiagų optimalius fotoelektrinius parametrus galimiems taikymams.

Disertacija yra sudaryta iš penkių skyrių, suskirstytų į smulkesnius poskyrius. Kiekvieno skyriaus pradžioje yra apžvelgiami aktualūs tyrimai ir problemos. Skyrių pagrindiniai rezultatai ir išvados yra pateikiamos kiekvieno skyriaus gale. Viso darbo išvados yra pateikiamos disertacijos pabaigoje. Bendras visuose skyriuose cituotos literatūros sąrašas yra pateikiamas darbo pabaigoje. Disertacijos pradžioje yra disertanto kartu su bendraautoriais publikuotų mokslinių straipsnių (tiek įtrauktų, tiek neįtrauktų į disertaciją), taip pat pranešimų konferencijose, kuriose pristatyti disertacijoje pateikti moksliniai tyrimai, sąrašas.

Pirmame disertacijos skyriuje yra pateikiama nepusiausvirųjų krūvininkų dinamikos ypatumų stipriai sužadintuose tiesiatarpiuose puslaidininkiuose apžvalga.

Antras skyrius, sudarytas iš trijų poskyrių, yra skirtas darbe naudojamų sužadinimo–zondavimo metodikų ir eksperimentinių duomenų analizės skaitmeniniu modeliavimu algoritmų apžvalgai.

Trečiame šio darbo skyriuje yra pateikiami InN sluoksnių su skirtingu pusiausvirųjų krūvininkų tankiu tyrimų rezultatai, naudojant skirtuminio pralaidumo (SP) ir šviesa indukuotų dinaminių gardelių (DG) metodikas. Pateikiami SP signalo gesimo trukmių kitimo rezultatai, keičiant zonduojančio pluoštelio bangos ilgį ir sužadinimo energijos tankį. Skaitmeniškai analizuojamos DG metodika išmatuotos difrakcijos efektyvumo kinetikos ir pateikiamos įvertintos netiesinės krūvininkų rekombinacijos koeficiento vertės. Šio skyriaus rezultatai yra publikuoti darbuose [P2–P5, P8].

Ketvirtas disertacijos skyrius, sudarytas iš trijų poskyrių, yra skirtas InGaN heterosandarų ir kvantinių sandarų su skirtingu In kiekiu tyrimams, naudojant SP ir DG metodikas. Pateikiama difrakcijos efektyvumo kinetikų gesimo trukmės analizė esant skirtingoms žadinančios energijos tankio vertėms ir bandinio temperatūroms. Aptariamos nepusiausvirųjų krūvininkų rekombinacijos ypatybės InGaN sluoksnyje su 13% In bei skaitmeninė kinetikų analizė. Pateikiamos krūvininkų difuzijos koeficiento ir gyvavimo trukmės verčių kitimo tendencijos, esant skirtingiems nepusiausvirųjų krūvininkų tankiams InGaN/GaN kvantinėse sandarose. Taip pat aprašomi sužadintų laidumo juostos būsenų relaksacijos spartos tyrimų rezultatai naudojant SP metodiką. Šio skyriaus rezultatai yra publikuoti darbuose [P1] ir [P7].

Penktame skyriuje yra pateikiami GaAsBi epitaksinių sluoksnių su skirtingu Bi kiekiu tyrimų rezultatai, naudojant DG metodiką. Apžvelgiamos nepusiausvirųjų krūvininkų gyvavimo trukmės ir difuzijos koeficiento temperatūrinės priklausomybės ir jų skaitmeninė analizė. Šio skyriaus rezultatai yra publikuoti darbe [P6].

Acknowledgement

I would like to give my special thanks to my scientific supervisor prof. Kęstutis Jarašiūnas for experessed trust, opportunity to improve my knowledge, inspiration and care.

I would like to thank prof. Artūras Žukauskas for the possibility to do the research work in the Institute of Applied Research.

Also I wish to thank dr. Mikas Vengris for helpful consultations and opportunity to do research work in the laboratory of Ultrafast–spectroscopy of VU Laser center.

I acknowledge dr. Ramūnas Aleksiejūnas, dr. Arūnas Kadys and dr. Tadas Malinauskas for valuable discussions, advices and sharing their experience on measurement equipment and experimental techniques.

Finally, I would like to thank my parents and my wife Viktoria for the patience and support in everyday life.

The work has been partially supported by the Lithuanian State Study Foundation and the Research Council of Lithuania.

List of abbreviations, used in the text

LED – Light Emitting Diode;

LITG – Light-Induced Transient Grating;

DT – Differential Transmission;

FCA – Free Carrier Absorption;

QW – Quantum Well;

MQW – Multiple Quantum Wells;

PL – Photoluminescence;

β–BBO – beta barium borate (BaB_2O_4) crystal;

YAG – yttrium aluminium garnet ($Y_3Al_5O_{12}$);

MBE – Molecular Beam Epitaxy;

MOCVD – Metal-Organic Chemical Vapour Deposition;

IQE – Internal Quantum Efficiency;

EQE – External Quantum Efficiency;

TMIn – trimetilindium ($In(CH_3)_3$);

TMGa –trimetilgalium ($Ga(CH_3)_3$).

Introduction

III-nitrides and their alloys are currently used in a variety of commercial optoelectronic devices, including green, blue, and ultraviolet light emitting diodes (LEDs) and lasers. However, the success in applications of group III-nitrides has been limited only to Ga-rich alloys. Despite the global success of III-nitrides, up to now Ga-rich InGaN LEDs faces the so called “efficiency droop” phenomenon, when brightness of LED vanishes at high current densities. This is a big issue in the development of high-efficiency LEDs suitable for solid state lightning. Several possible reasons were proposed including Auger recombination, polarization-field assisted electron leakage, carrier delocalization and nonradiative recombination at defects as droop-causing mechanisms in InGaN LEDs. However, there is no agreement yet as to be the main reason causing nonradiative losses in high power LEDs and needs further studies.

Much less effort has been devoted to InN and In-rich InGaN. Early studies of InN interband optical absorption resulted in a fundamental energy bandgap of ~2 eV. This value of the bandgap was widely accepted and frequently used as the end-point value for the extrapolation of crystal properties in InGaN alloys. Recent improvements in growth technologies have led to better crystalline quality of InN films and energy bangap value of about 0.64 eV, revealing uncertainty on earlier accepted properties of In-rich InGaN alloys. Despite the better quality of InN crystals, the electrical properties still remain under investigation. The potential of extending the bandgap energies of the group III-nitrides into the long wavelength region has generated considerable interest of research groups worldwide. It was discovered that alloying GaN with InN has a detrimental effect on electrical and optical properties of the resulting alloys with high In content. The difficulties in fabricating high-quality InGaN crystals with large In-content remains a major problem in visible spectrum LEDs manufacturing. Epitaxial InGaN films with high In-content are also important for photovoltaics, while cell’s efficiency from one type material approaches the Schokley-Quisser theoretical limit and to overcome this value tandem solar cells are needed. Considering difficulties mentioned above there are huge interest on experimental studies of structural, optical and electrical properties of InN and In-rich InGaN alloys.

The ongoing developments of semiconductor devices force to look up for new materials with tailored optical and electrical properties. A few examples of applications that require semiconductor materials with new properties are high efficiency solar cells, light emitting materials with independent on temperature output wavelengths, low power consumption transistors for wireless devices, safety systems based on THz radiation properties, and new kinds of materials that allow the manipulation of electron spins. The dilute bismide GaAsBi ternary alloys can potentially contribute to development of ultrafast optoelectronic detectors or emitters. As the GaAsBi system is quite new, there are a lot of unexplored electrical and structural properties important for possible applications. For example, it is known that the valence band is affected with Bi alloying but there are lack of experiments on properties of nonequilibrium holes in GaAsBi.

Keeping in mind issues mentioned above the thesis was aimed for investigation of carrier dynamics in new semiconductor materials by optical means. The **main goal** of the thesis were to gain a new knowledge on excess carrier dynamics by using optical time-resolved pump-probe techniques in new perspective materials with technologically variable properties for semiconductor electronics and optoelectronics – InN, InGaN, and GaAsBi heterostructures. The experimental studies in a wide range of excess carrier density (10^{18}–10^{20} cm^{-3}) and temperature (10–300 K) were targeted to determine the dominant carrier recombination channels, to identify interplay between radiative and nonradiative recombination processes, and to clarify the role of localization to nonequilibrium carrier recombination and diffusion processes, thus finding optimal photoelectrical parameters of semiconductor materials for applications.

Main objectives

To determine excess carrier lifetime and diffusion coefficient values at different experimental conditions (photo-excited carrier density, sample temperature) in MBE-grown InN layers with different background carrier density. To determine dominant excess carrier recombination and scattering mechanisms at room temperature by performing numerical modeling of experimental data.

To determine role of localization to excess carrier recombination rate and diffusion processes in InGaN layers and multiple heterostructures. To identify interplay between radiative and nonradiative excess carrier recombination in different spectral

regions. To investigate dependence of excess carrier recombination rate on excitation fluence and temperature. To analyze dominant excess carrier recombination mechanisms and determine their coefficients by numerical modeling of experimental data.

To investigate excess carrier dynamics in GaAsBi layers with different Bi content and evaluate an impact of Bi concentration to carrier recombination rate and diffusivity of nonequilibrium holes by using light-induced transient grating technique.

Novelty and significance of the thesis

Recombination rate of excess carriers in MBE-grown InN layers was investigated at experimental conditions enabling nonequilibrium free carrier absorption detection. The experimental data allowed to propose a new trap-assisted nonradiative Auger recombination mechanism in highly excited InN.

Dependencies of excess carrier lifetime τ and diffusion coefficient D on In content, sample temperature, and excess carrier density were determined in MOCVD-grown Ga-rich InGaN epitaxial layer and InGaN/GaN multiple quantum wells and MBE-grown In-rich InGaN layers. A correlation between D and τ values due to delocalization of photo-excited carriers was determined. The injection-activated radiative and nonradiative recombination coefficients were determined in InGaN alloys by numerical modeling of experimental data.

Dependencies of nonequilibrium hole diffusion coefficient and excess carrier recombination rate on Bi content and sample temperature were determined by optical means in MBE-grown GaAsBi layers.

Points to be maintained (statements to defend)

1. Free carrier absorption in optical transparency region and diffraction efficiency kinetics in the vicinity of absorption edge of InN are not affected by carrier intraband repopulation in the conduction/valence bands and thus allow to determine carrier lifetime and its dependence on excess carrier density.

2. Trap-assisted Auger recombination is the dominant excess carrier recombination mechanism at room temperature in MBE-grown InN layers with background carrier density in range n_0=(1.4–4.7)×10^{18} cm^{-3}.

3. The increasing excess carrier recombination rate in a single MOCVD-grown $In_{0.13}Ga_{0.87}N$ layer with increase of carrier density in range (ΔN=10^{18}–10^{20} cm^{-3}) and decrease of temperature (in 295–100 K range) is governed solely by radiative recombination which coefficient at room temperature equals to $B_{T=300K}$=7×10^{-11} cm^3/s.

4. Both nonradiative and radiative recombination contribute to an increase of excess carrier recombination rate at high photo-excited carrier density in MOCVD-grown $In_xGa_{1-x}N$ (0.16>x>0.034) multiple quantum wells.

5. Bi-induced potential fluctuations determine the tenfold decrease in nonequilibrium hole mobility (down to 10–20 cm^2/(V·s)), comparing to GaAs, in the MBE-grown $GaAs_{1-x}Bi_x$ (0.063>x>0.025) layers.

Layout of the thesis

The thesis consists of five chapters. The articles and conference contributions of the author together with co-authors are listed at the beginning of the thesis. The thesis is finalized by the conclusions. The layout of the thesis is organized as follows.

The **first chapter** is devoted to nonequilibrium carrier dynamics in highly excited direct bandgap semiconductors.

Chapter 2. Time-resolved optical techniques for investigation of carrier dynamics

2.1 Differential transmission technique

The experimental setup scheme of differential transmission (DT) measurements is shown in the Fig. 2.1. For a sample excitation and probing we used two optical parametric amplifiers pumped by 120 fs pulse Ti:sapphire laser system working at 1 kHz.

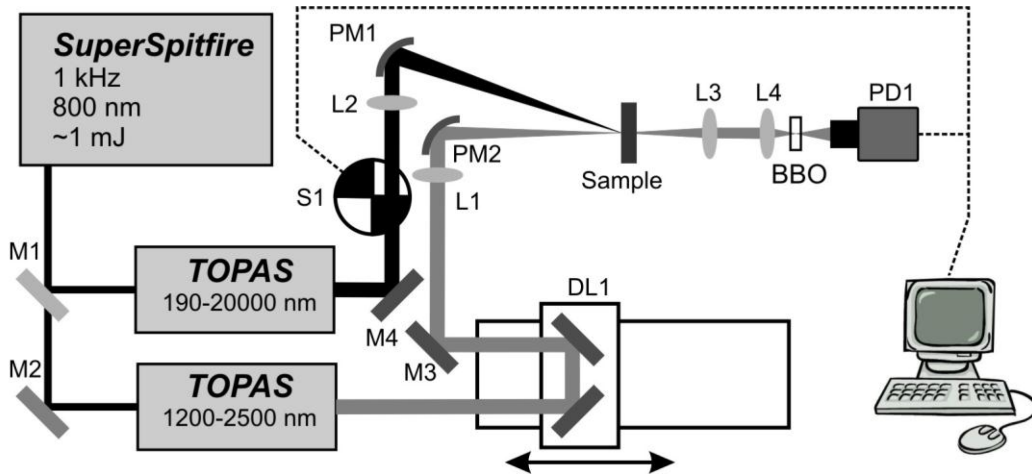

Figure 2.1. Experimental setup scheme of differential trasmission measurements.

Time-resolved differential transmission (DT) technique is based on measurements of light-induced absorption change $\Delta\alpha(t)$. In this work, the $\Delta\alpha(h\nu, t)$ evolution at fixed wavelengths was estimated by measuring a ratio between the sample transmission with pump $T(t)$ and without pump T_0 for a probe beam with varying delay time t:

$$T(t) = T_0 \cdot \exp[-\alpha(h\nu,t)\cdot d] \rightarrow \alpha(h\nu,t)\cdot d = -\ln\left[\frac{T(t)}{T_0}\right], \qquad (1)$$

where d is the sample thickness. The characteristic decay time is the time it takes for signal to drop $1/e$ times.

2.2 Light-induced transient grating technique

This section is dedicated to implementation of Light-Induced Transient Grating (LITG, or dynamic grating, DG) technique for investigation of carrier dynamics. The main principle of LITG technique is to excite a transient grating in a material using the interference of two pump beams and to scan the decay of the grating by measuring the diffraction efficiency of the third (probe) beam. For the dynamic grating writing on the sample we used the interference pattern of the first (1064 nm), second (532 nm) or third (355 nm) harmonic of 25 ps pulse YAG:Nd^{+3} laser. The spatio-temporal evolution of created free carrier spatial modulation was probed by diffraction of a delayed (up to ~4ns) probe beam at 1064 nm. In order to extend probe beam wavelength to IR region optic parametric generator (OPG) pumped by 3rd harmonic (355 nm) of YAG:Nd^{+3} was used. The experimental setup scheme of LITG measurements is shown in Fig. 2.2.

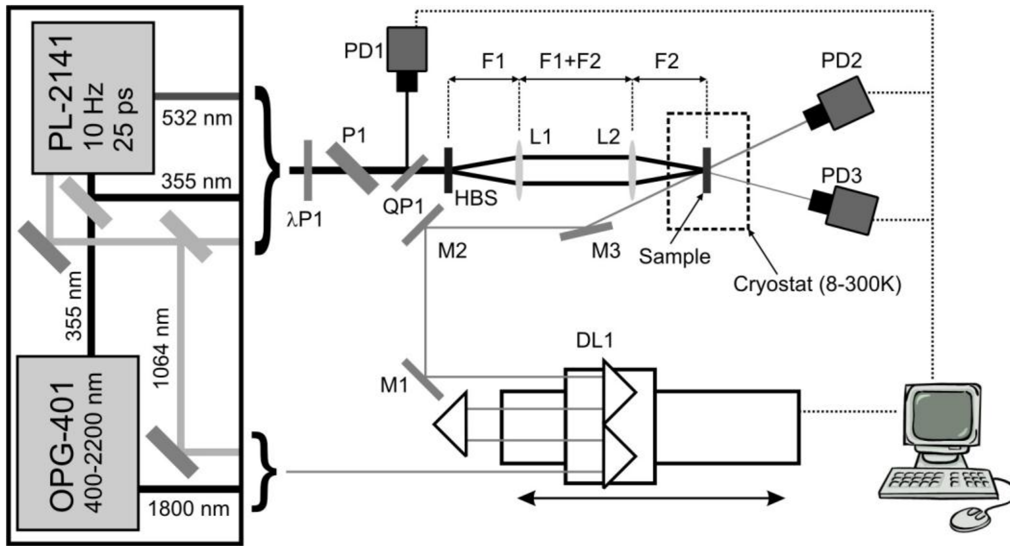

Figure 2.2. Experimental setup scheme of LITG measurements.

The decay of excited grating is probed by measuring the grating diffraction efficiency η, which is equal to the ratio of diffracted I_D and transmitted part I_T of the probe beam:

$$\eta = \frac{I_D}{I_T} = \left|J_1(\phi)\right|^2 \approx \left|\frac{\pi \Delta \tilde{n} d}{\lambda}\right|^2 = \left(\frac{\pi \Delta n d}{\lambda}\right)^2 + \left(\frac{\Delta \alpha d}{4}\right)^2, \qquad (2)$$

where J_1 is the first order Bessel function, $\phi = \pi \Delta \tilde{n} d$, Δn and $\Delta\alpha$ – refractive index and absorption coefficient change, respectively, d – dynamic grating thickness. The experiments presented in the thesis where obtained when the rule $\Delta n > \Delta\alpha$ holds, and the

probe beam diffracts on the grating due to refractive index change modulation by the free-carriers, $\Delta n = n_{eh}\Delta N$ (n_{eh} is refractive index change by one electron-hole pair, ΔN – nonequilibrium carrier density). The decay time of grating efficiency corresponds to the time interval $t=\tau_G$ in which the η value decreases by e^2 times,

$$\eta(t) \propto \exp\left(-\frac{2t}{\tau_G}\right). \tag{3}$$

The excited dynamic grating decays in time due to carrier diffusion and recombination. The advantage of LITG technique is that carrier recombination and diffusion processes can be separated by measuring dynamic grating decay time τ_G dependence on grating period Λ as latter has dependence

$$\frac{1}{\tau_G} = \frac{1}{\tau_R} + \frac{1}{\tau_D} = \frac{1}{\tau_R} + \frac{4\pi^2 D}{\Lambda^2}, \tag{4}$$

where τ_R is the excess carrier recombination time, D is the diffusion coefficient.

2.3 Numerical modeling of carrier dynamics

The modeling of excess carrier dynamics was performed by numerically solving a differential continuity equation

$$\frac{\partial N(x,z,t)}{\partial t} = \nabla[D\nabla N(x,z,t)] - \frac{N(x,z,t)}{\tau_R} - BN^2(x,z,t) - CN^3(x,z,t) + G(x,z,t), \tag{5}$$

with boundary conditions:

$$\left.\frac{\partial N(x,z,t)}{\partial z}\right|_{z=0} = \frac{S_1}{D}N(x,0,t), \quad \left.\frac{\partial N(x,z,t)}{\partial z}\right|_{z=d} = -\frac{S_2}{D}N(x,d,t), \tag{6}$$

where B and C are bimolecular and Auger recombination rates, respectively, S_1 and S_2 are surface recombination velocities at the front and back surfaces, G(x,z,t) is carrier generation function, and d is sample thickness. More detailed description of numerical modeling algorithm can be found in the Chapter 2.3 of the thesis.

Chapter 3. Nonequilibrium carrier dynamics in InN layers with different background carrier density

3.1 Investigation of carrier recombination by time-resolved DT technique

The differential transmission measurements were carried out in four InN layers with different background carrier concentration n_0 grown by molecular beam epitaxy (MBE) on c-plane sapphire with GaN or AlN buffer layer (n_0=1.4×10^{18} cm^{-3} in the sample #1, n_0=2.1×10^{18} cm^{-3} in the sample #2, n_0=3.5×10^{18} cm^{-3} in the sample #3 and n_0=4.7×10^{18} cm^{-3} in the sample #4). The investigated samples were provided by the technological centers from the USA, Japan, and Germany. Photo-excited carriers were created by excitation at 1000 nm (using 120 fs duration laser pulses), while the probe wavelength varied from 1550 (0.8 eV) to 2300 nm (0.54 eV).

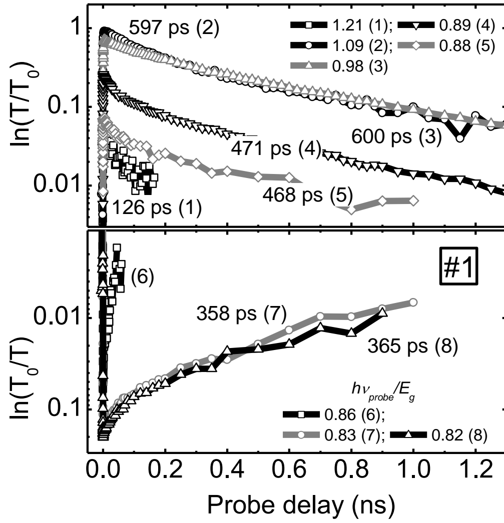

Figure 3.1. Differential transmission transients at constant pump fluence and various probe photon energies in the sample #1.

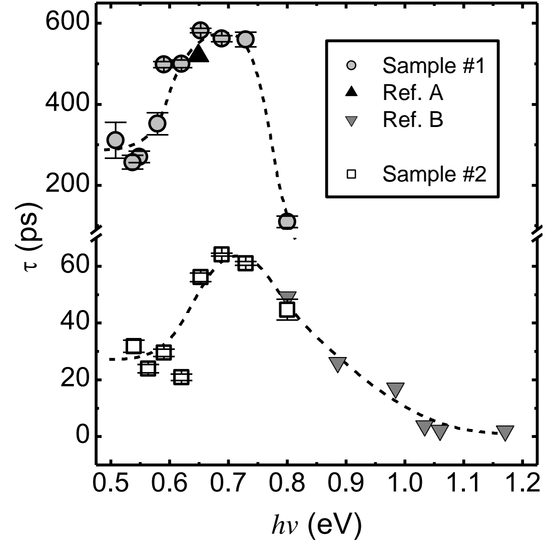

Figure 3.2. Recovery time of DT signal vs probe photon energy for the samples #1 and #2. For comparison, complementary data of optical bleaching recovery time in the same InN samples are given in the plot (Ref.A – [1], Ref.B – [2]). Dashed lines are guides to an eye.

By decreasing probe quanta energy $h\nu_{pr}$, a gradual transfer from optical bleaching (then absorption coefficient change $\Delta\alpha<0$) to the induced absorption ($\Delta\alpha>0$ at $h\nu_{pr}\geq0.55$ eV in sample #1) was observed, while in the intermediate spectral region the induced bleaching and darkening nearly cancelled each other (curve 6 in Fig. 3.1). The induced absorption well below the absorption edge was attributed to free carrier

absorption (FCA) because the signal was increasing linearly with excitation fluence and no defect-related absorption was observed in this spectral region. The FCA signal was proportional to the total density of free carriers; therefore, its relaxation provided the carrier lifetime, which was ~360 ps in the sample #1. The bleaching recovery time at the bottom of E_g was longer than the FCA decay time, measured under the same excitation conditions. This peculiarity suggests that the dynamics of these optical nonlinearities is driven by different physical mechanisms and the bleaching kinetics close to E_g reflects more complicated processes than the commonly accepted "band-to-band" recombination [1, 3]. While the FCA signal carries information about free electrons in all k-states in the conduction band, the induced bleaching is only sensitive to the probed states. Probing at, or slightly below, E_g follows the states at the bottom of the conduction band and in the defect-related band-tails. The re-population rate of these states is apparently different from the decay of total excess electron density. In particular, the recovery of bleaching kinetics slightly below E_g could be attributed to "free-to-band" recombination of electrons at the bottom of the conduction band with the holes in the valence band-tails [4]. Low density of localized states in the tails results in slower recombination rate, and, therefore, slower decay of the optical bleaching at corresponding wavelengths. The same

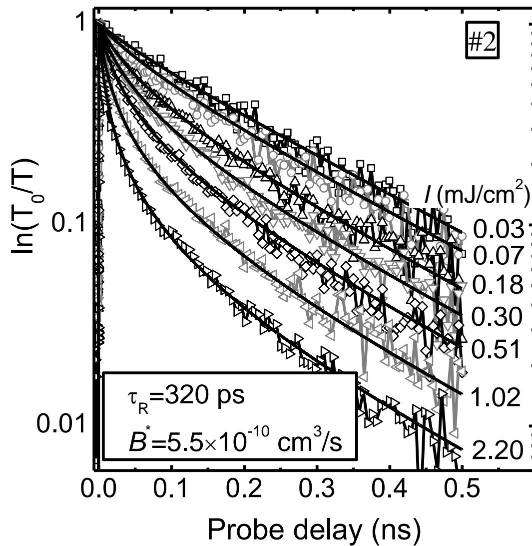

Figure 3.3. Kinetics of FCA decay in the sample #2 at various excitation fluences: experimental data (points) and numerical fitting (lines) using Eq. 5. The numerically determined recombination coefficient B^* and carrier lifetime τ_R are given in the plot.

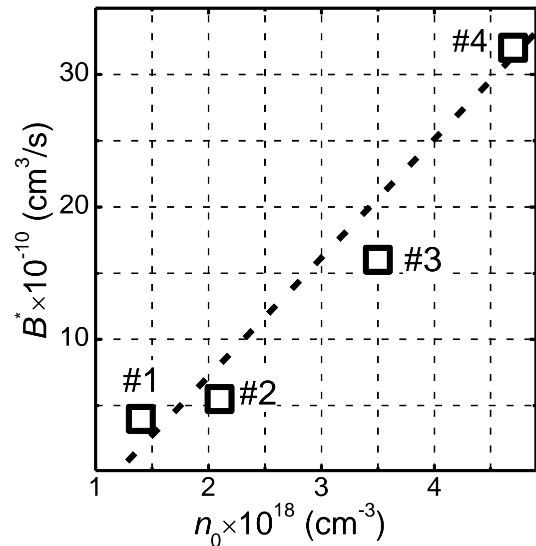

Figure 3.4. Nonlinear recombination coefficient B^* value dependence on background carrier density in the sample.

tendency of DT transients was observed In the sample #2 except the faster DT relaxation times due to higher background electron density (and probably higher defect density) in the sample (see Fig. 3.2).

The injection-enhanced recombination rate was observed in all InN layers by measuring FCA kinetics at 2300 nm probe and varying the excitation fluence (see Fig. 3.3). In order to reveal dominant recombination mechanism we numerically solved the carrier continuity equation (Eq. 5). The parameters corresponding to the best fit of experimental data are summarized in the Table 3.1 (next section). The dependence of carrier recombination rate on the total carrier density $1/\tau \propto B^*(n_0+\Delta N)$ was found the same as for interband radiative recombination, $1/\tau = B\Delta N$. However, the determined value of B^* was at least one order of magnitude larger than the interband recombination rate in InN ($B=3\times10^{-11}$ cm^3/s at 300K [3]). Moreover, nonlinear coefficient B^* value was found dependent on background carrier density in the sample (see Fig. 3.4).

3.2 Investigation of carrier recombination and diffusion dependence on temperature by using LITG technique

To further elucidate the recombination mechanisms measurements using LITG technique was performed. The decay rate of room temperature diffraction efficiency kinetics in the samples #1 and #2 was found dependent on photo-injected carrier density and followed the relationship $1/\tau = B^*(n_0+\Delta N)$. Subsequent numerical modeling of η kinetics provided the same carrier lifetime and nonlinear recombination coefficient B^* as for FCA kinetics (Fig. 3.5 and Fig. 3.3).

In order to reveal the nature of the observed nonlinear recombination in InN layers the investigation of η decay rate dependence on temperature was performed. In Fig. 3.6 we show comparison of experimentally obtained diffraction efficiency kinetics (dots) in the sample #2 with numerically calculated ones, assuming that B^* value is radiative recombination coefficient (dashed lines). Studies of carrier dynamics at lower temperatures revealed that nonlinear decay rate was not becoming faster with decreasing temperature, as it expected for the radiative recombination with well-known dependence, $B \propto T^{-3/2}$ in nitrides [5]. In contrary, the decay kinetics at lower temperature has shown a

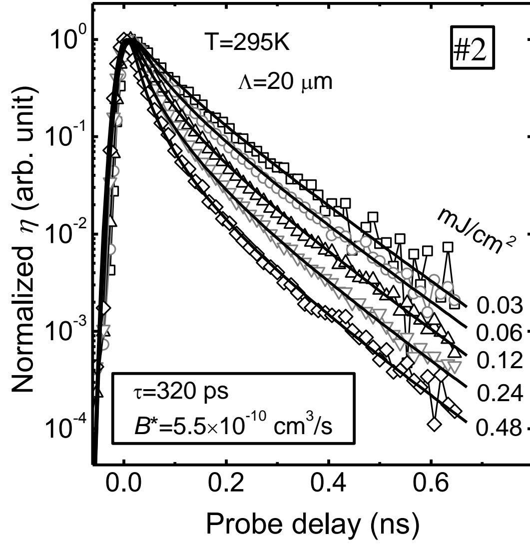

Figure 3.5. Normalized room temperature diffraction efficiency kinetics at different excitation fluence in the InN sample #2.

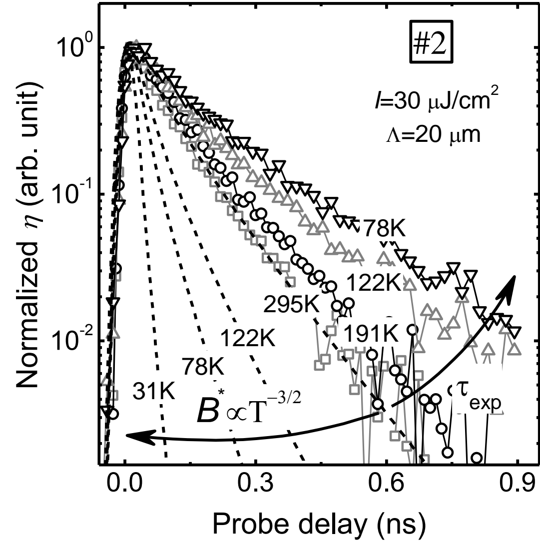

Figure 3.6. Comparison of experimentally obtained diffraction efficiency kinetics (dots) in the sample #2 with numerically calculated ones, assuming that B^* value is radiative recombination coefficient (dashed lines).

tendency of slower decay in 130–70 K. The same tendency of diffraction efficiency decay also was found in the sample #1.

The observed increase of carrier recombination rate with increasing excess carrier density and its temperature dependence, which does not support radiative recombination law as well the B^* value dependence on background carrier density n_0 allowed us to propose a trap-assisted Auger recombination (TAAR) being the dominant excess carrier recombination channel in the InN at room temperature. The density of traps N_T is known to vary in the InN samples proportionally to n_0 [4, 6, 7] thus assuming that $n_0 \approx N_T$, we determined the TAAR coefficient $C_{TAAR} = B^*/N_T = (4.5\pm2)\times10^{-28}$ cm^6/s.

Table 3.1. Summary of numerically determined τ_R, B^*, C and C_{TAAR} values in investigated InN samples.

Sample No.	n_0 (cm^{-3})	τ_R (ns)	B^* (cm^3/s)	C (cm^6/s)	C_{TAAR} (cm^6/s)
#1	1.4×10^{18}	1.45	4×10^{-10}	–	2.8×10^{-28}
#2	2.1×10^{18}	0.32	5.5×10^{-10}	–	2.6×10^{-28}
#3	3.5×10^{18}	0.8	16×10^{-10}	10^{-29}	4.6×10^{-28}
#4	4.7×10^{18}	0.12	32×10^{-10}	–	6.4×10^{-28}

Chapter 4. Nonequilibrium carrier dynamics in InGaN heterostructures with different In content

4.1 Investigation of carrier recombination by using transient gratings technique in $In_xGa_{1-x}N$ layers with In content x>0.7

In this section the study of MBE grown ~0.6 µm thick In-rich $In_xGa_{1-x}N$ layers with In content 0.9>x>0.7 using LITG technique is presented. At 532 nm photo-excitation and 1064 nm probe, the decreasing grating decay time indicated an increasing excess carrier recombination rate for alloys with higher Ga content. The longest lifetime of about 180 ps was found in the layer with x=0.9. Moreover, the refractive index modulation by free carriers (Δn_{FC}<0) competed with temperature-induced (Δn_T>0), revealing a dip in the diffraction kinetics at $|\Delta n_{FC}| = |\Delta n_T|$ and subsequent long lasting decay component due to light diffraction on thermal grating. The latter effect dominated in a layer with the largest bandgap and pointed out that the main reason of the lattice heating is not the excess energy of pump beam photons (which was the highest for pure InN), but the rate of non-radiative recombination, being fastest in the sample with In content x=0.7 (see Fig. 4.1). Taking into account the latter experimental observations, for the excess carrier photo-excitation we used 1st YAG:Nd laser harmonic (1064 nm) while probe wavelength was set to 1500 nm using an OPG.

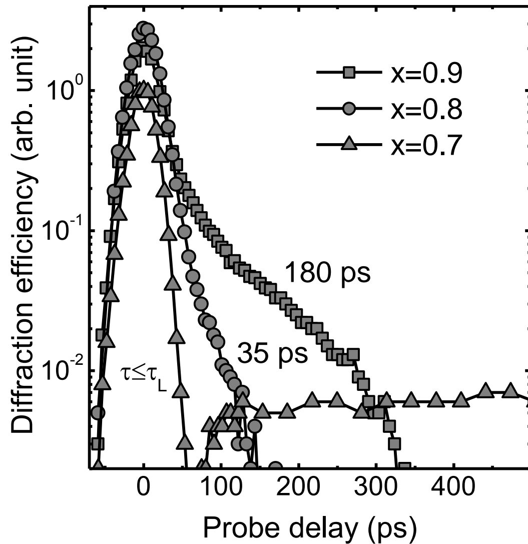

Figure 4.1. Kinetics of free-carrier grating with subsequent formation of a thermal grating (excitation at 532 nm).

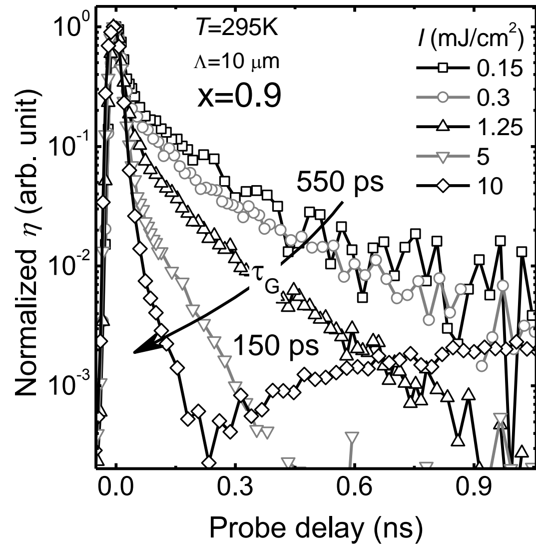

Figure 4.2. Diffraction efficiency kinetics at different excitation fluences with subsequent thermal grating effect at the highest injection (excitation at 1064 nm).

The measurements at room temperature in a wide excitation range (Fig. 4.2) revealed that recombination rate is weekly dependent on excess carrier density and may lead to thermal grating as well. The similar tendency of $\tau_G(\Delta N)$ was found at 10 K, while the τ_G value increased and varied in range from 6 ns to 1.6 ns for excitation range 0.15–10 mJ/cm^2.

A set of grating decay kinetics has been measured at the same excitation conditions but varying the sample temperature (Fig. 4.3 a)). We found that the grating decay rate is ruled by the thermal activation, and the determined value of 19 meV (Fig. 4.3 b)) can be assumed as the activation energy ΔE for carrier recombination. The

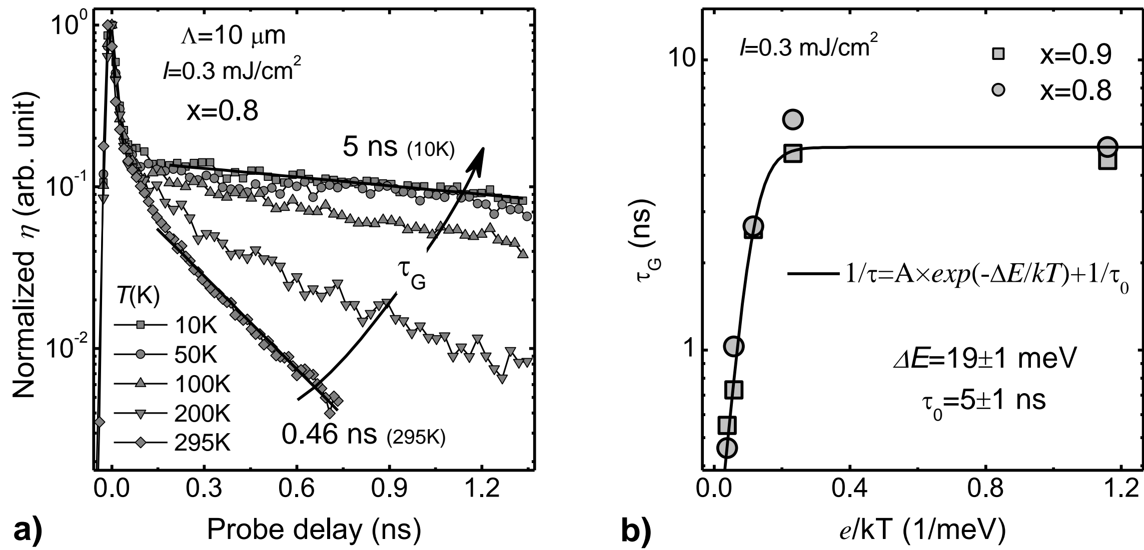

Figure 4.3. a) Diffraction efficiency kinetics at different temperatures, b) grating decay time dependence on reciprocal thermal energy.

origin of the potential barriers can be: i) InGaN bandgap fluctuations due to inhomogeneous distribution of In or Ga atoms in the alloy [8, 9]; or ii) bandgap fluctuations due to space-charge region around charged dislocations [10]. In both cases, photo- or thermal activation is needed to overcome the local potential barrier and recombine.

4.2 Investigation of excess carrier recombination rate dependence on excitation fluence and temperature in the $In_xGa_{1-x}N$ layer with x=0.13

The present section is focused on the study of carrier recombination rate dependence on excitation fluence and temperature in MOCVD-grown 50-nm-thick $In_{0.13}Ga_{0.87}N$ layer. The sample was grown by the AIXTRON reactor in Aachen

(Germany) on c-plane sapphire substrate. The dynamic grating on the sample was created using 3rd harmonic (355 nm, $h\nu$=3.49 eV) of 25 ps pulse YAG:Nd^{+3} laser taking into account the bandgap value of investigated InGaN alloy (PL emission peak was at 2.9 eV). The grating decay was probed by a delayed probe beam at 1064 nm.

Room temperature diffraction efficiency kinetics revealed increasing with excitation excess carrier recombination rate (Fig. 4.4). The expected diffusive decay time τ_D (Eq. 4) at given grating period Λ=12 μm and taking D=2 cm^2/s (typical value for GaN [11, 12]) equals to 16 ns, being much longer than the observed decay time. Thus grating decay time τ_G at the given experimental conditions represents carrier recombination time. The saturation of diffraction efficiency dependence on excitation (Fig. 4.5) at 0.18 mJ/cm^2 showed a threshold of stimulated emission. The stimulated recombination acts as a very fast recombination channel, which takes place during the pump pulse and reduces carrier density to the threshold value. The contribution of stimulated recombination was also observed by complementary time-resolved photoluminescence measurements. At reaching these conditions, impact of InGaN to diffraction saturates and the subsequent increase of η is due to the underlaying 2 μm-thick GaN buffer layer (see curves in Fig. 4.5 at I>0.3 mJ/cm^2). Extrapolation of $\eta(I)$ of GaN to the low

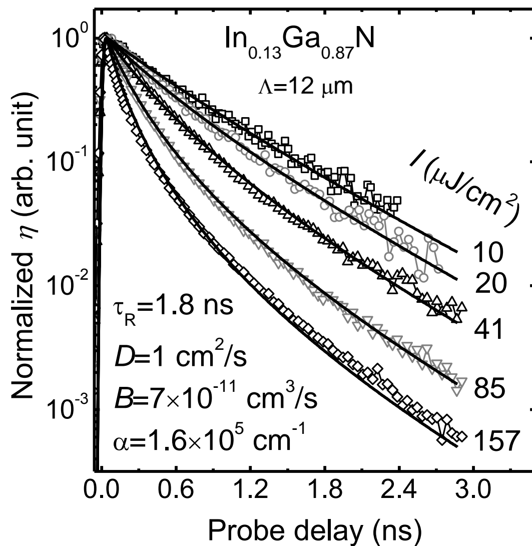

Figure 4.4. Room temperature diffraction efficiency kinetics at different excitation fluence. Solid lines indicates numerically calculated fits with parameters given in the legend.

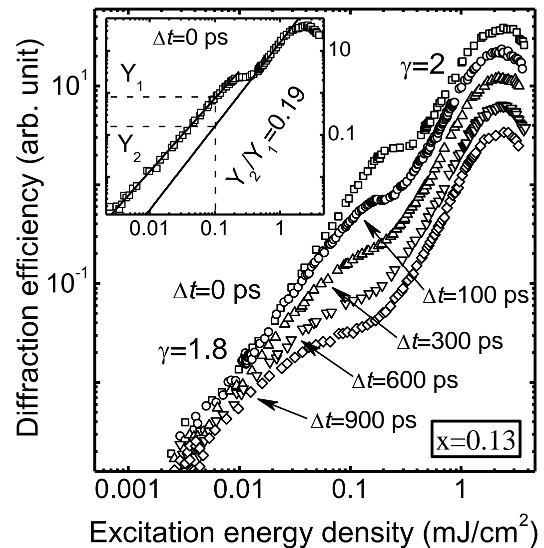

Figure 4.5. Diffraction efficiency dependence on excitation fluence at different probe delays. The inset shows contribution of InGaN layer and GaN buffer to η at zero delay time.

injection regime (see inset in Fig. 4.5) provides ratio of the InGaN and GaN contribution to η at zero delay. The ratio value allowed us to determine the absorption coefficient value $\alpha_{355\ nm}=1.6\times10^{5}\ cm^{-1}$ for the InGaN layer at the pump wavelength. Gradually decreasing slope value γ for InGaN $\eta(I)$ dependences at longer delay time and excitations bellow the stimulated recombination threshold (see range 5–100 μJ/cm^2 in Fig. 4.5) points out that average carrier lifetime in InGaN is dependent on injected carrier density.

Data of temperature-dependent carrier lifetime and diffusivity in InGaN layer are summarized in Fig. 4.6. Set of LITG decay curves for different grating periods were measured and from their exponential tails the values of D and τ_R using Eq. 4 were determined. A strict inverse correlation between increasing with T lifetime ($\tau_R \propto T^{1/2}$) and decreasing bipolar diffusion coefficient ($D \propto T^{-1/2}$) clearly indicated that carrier diffusion

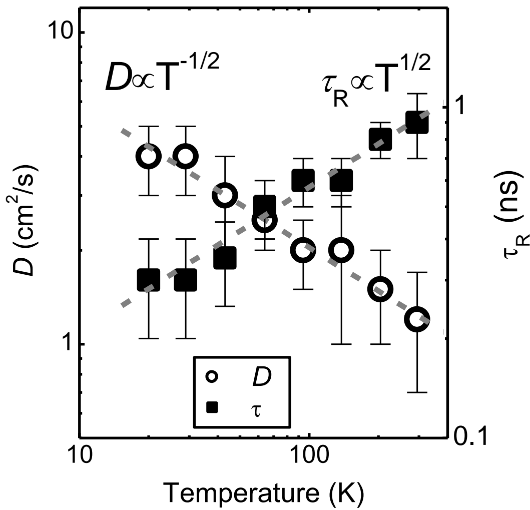

Figure 4.6. Carrier lifetime and diffusion coefficient dependence on temperature.

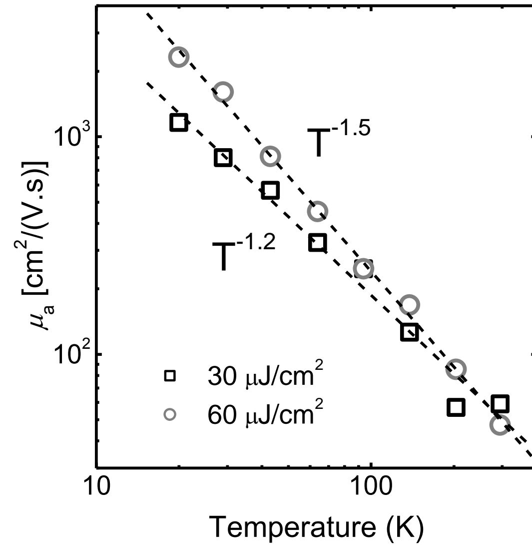

Figure 4.7. Ambipolar mobility dependence on temperature at different excitation fluences.

flow to defects determines the lifetime (similarly to low-defective GaN layers and bulk crystals, where the linear dependences were observed verifying diffusion-governed carrier recombination at dislocations, positioned at hexagon grain boundaries ([13, 14]). The mobility dependence (Fig. 4.7) followed relationship $\mu \propto T^{-3/2}$ (scattering by acoustic phonons), while at twice lower injections this dependence indicated lower mobility and lower its slope on T (i.e. impact of additional scattering presumably by charged defects).

The observed tendencies imply that screening of the defects by excess carriers may take place and lead to enhanced diffusivity and shorter lifetimes, when injection level of few times 10^{18} cm^{-3} is reached. We note that experimentally we did observe decreasing with excitation lifetime at room temperature but not an increase of D *verus* ΔN (D value was 1.1±0.2 cm^2/s while ΔN varied in the range 10^{18}–10^{19} cm^{-3}). The expected increase of D was probably opposed by bandgap narrowing which diminishes the diffusivity.

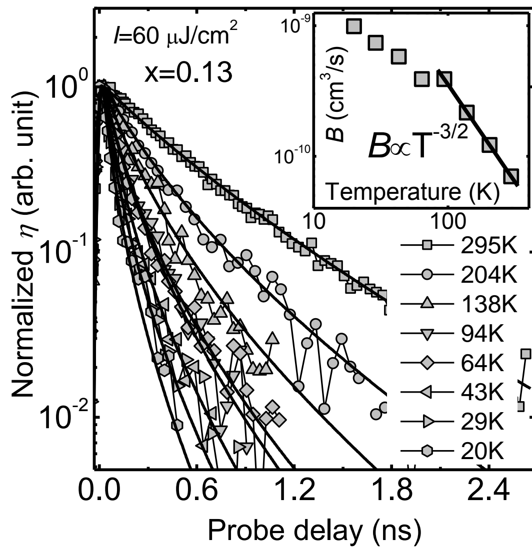

Figure 4.8. Diffraction efficiency kinetics at different sample temperature. Inset shows B value dependence on temperature determined from numerical modeling results (solid lines).

The final step was numerical fitting of the experimentally measured LITG decay kinetics at various sample temperatures (Fig. 4.8). The determined B value at room temperature was 7×10^{-11} cm^3/s (see Fig. 4.4) and its temperature dependence followed well-known relationship $B \propto T^{-3/2}$ (see inset in Fig. 4.8), thus confirming that the dominant recombination mechanism in $In_{0.13}Ga_{0.87}N$ layer at high photo-injected carrier densities is a radiative recombination.

4.3 Investigation of excess carrier dynamics in $In_xGa_{1-x}N$ MQW layer with different In content ($0.16>x>0.034$)

In this section the study of excess carrier diffusivity and lifetime dependence on excitation and In content and in InGaN/GaN MQW is presented. The investigated samples consisting of ten periods of ~4 nm-thick InGaN QW and 8 nm-thick GaN barriers were grown on c-plane sapphire by the scientist of Vilnius University using MOCVD reactor. Different In content in InGaN well was achieved by varying the ratio of metal-organic precursors TMIn/TMGa. The reference In-free sample grown under the same growth conditions also was investigated. In content in the InGaN/GaN MQW was determined from time-integrated PL spectra line under pulsed excitation at 266 nm and 0.7 mJ/cm^2 pump fluence.

To investigate transport and nonlinear recombination of excess carriers, we recorded LITG kinetics in each sample at several excitation energy fluencies, varying within 0.05–1 mJ/cm^2 range. In addition, LITG kinetics were measured for several periods of transient grating, which allowed us determination of effective carrier lifetime τ and diffusivity D using Eq. 4. It is worth to note, that experimentally obtained effective lifetime τ_{eff} reflects an intermixture of several recombination processes and thus may differ from the linear carrier lifetime τ_R, which is caused by carrier recombination through defects. For example, LITG decay in the reference GaN layer was single-exponential within 0.05–0.5 mJ/cm^2 range and provided 0.9 ns nonradiative carrier lifetime. In contrast, experimentally measured LITG kinetics in InGaN with 10.8% of In (filled symbols in Fig. 4.9 b)) are strongly excitation-dependent. Nevertheless, at the lowest excitations the decay in InGaN alloys was nearly exponential, and the slow decay tails provided the effective lifetime τ_{eff} value. Measurements in the latter conditions on InGaN samples with x=0.034, 0.108 and 0.15 of In provided values of τ_{eff} and D, varying with In content and dependent of excitation fluence (Fig. 4.9 a)).

LITG kinetics in all InGaN layers become increasingly non-exponential with excitation, with the initial component decaying faster at higher carrier densities; this tendency was found stronger pronounced in QWs with higher In content. Such a

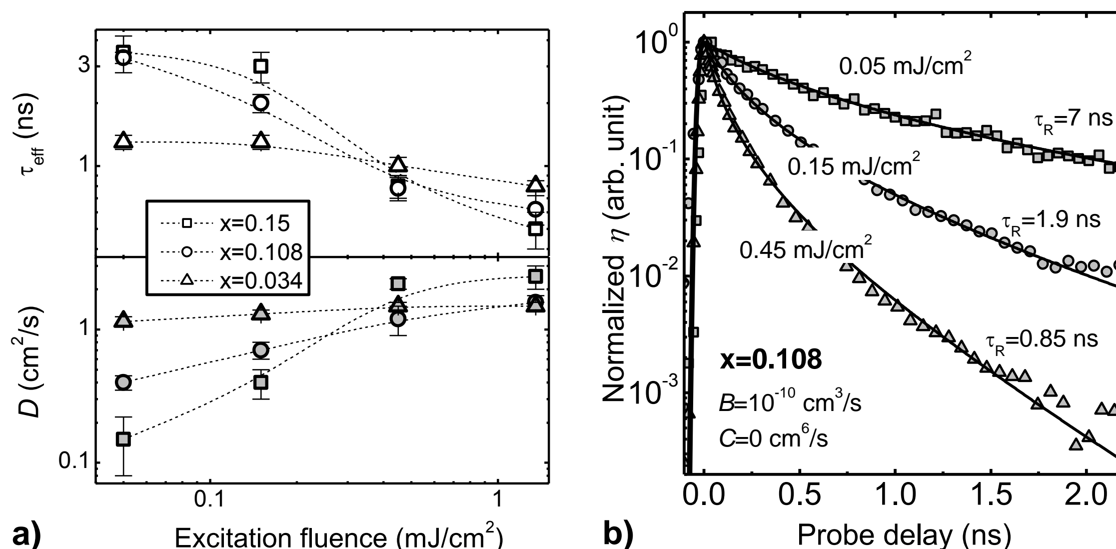

Figure 4.9. a) Dependence of carrier diffusivity and effective lifetime on excitation fluence in InGaN/GaN MQW with different In content (dashed lines ar guide to an eye); b) diffraction efficiency kinetics at different excitation fluences in InGaN/GaN MQW sample with 10.8% of In.

behavior is a typical fingerprint of nonlinear recombination processes, thus we modeled spatial and temporal distribution of excess carriers using continuity equation (Eq. 5). In Fig. 4.10 we show numerically determined τ_R (a) and B (b) coefficients. Here τ_R will be called nonradiative carrier lifetime, which reflects the rate of carrier recombination through the defects. Carrier lifetime, both determined numerically τ_R and experimentally τ_{eff} (see Figs.4.9 a) and 4.10 a)) (i) increase with In content, especially at low excitation densities, and (ii) drops with excitation. Such a tendency is non-typical for carrier recombination through defects, where the lifetime should be constant or increase with the carrier density, if the traps get filled. In addition, D shows a nonlinear behavior with excitation as well. At low carrier densities, D drops from 1.5 cm^2/s down to 0.1 cm^2/s when x increases from 0.034 to 0.15. When excitation is increased, D increases and difference between samples gradually vanishes (Fig. 4.9 a)). These tendencies were explained using a model of localized and free carriers. At relatively low carrier density, a bigger part of particles are spatially localized in potential minima caused by fluctuations of In composition and QW thickness; in addition, electrons and holes are separated by internal electrical field in QW. Localized carriers have low mobility and this is reflected in small carrier diffusivity of such a system. Localization hinders also the nonradiative recombination, as electrons and holes are not able to reach recombination sites, thus the lifetime remains long. As carrier density (or excitation) increases, relatively more

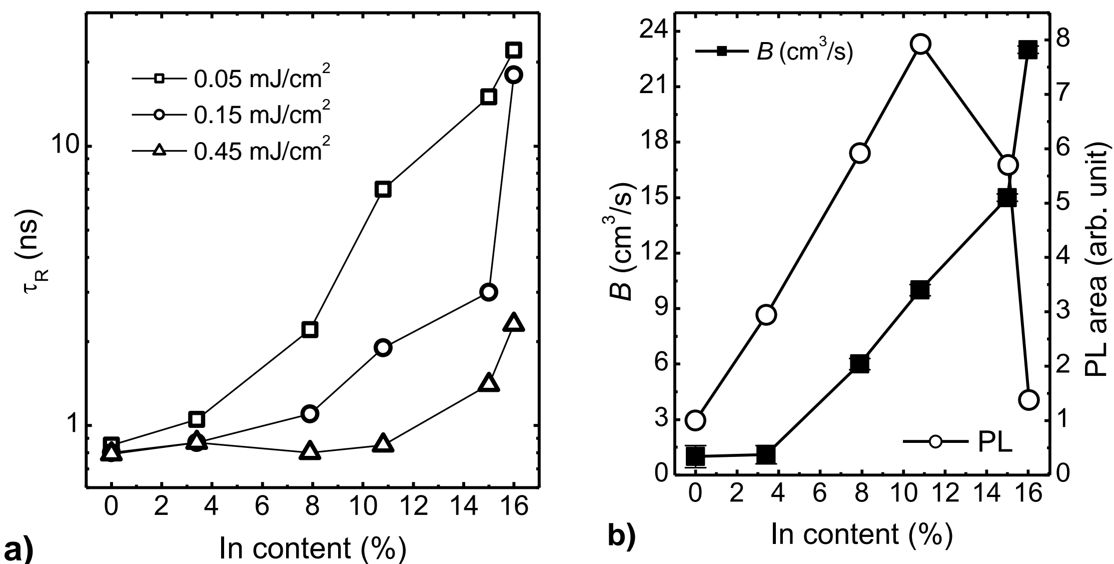

Figure 4.10. a) Numerically calculated τ_R values as a function of In content for three excitation fluences; b) B value (filled squares) and spectrally integrated PL signal (pump 266 nm, 0.7 mJ/cm^2, open circles) as a function of In content in the samples.

carriers become delocalized as the localized states become filled, thus diffusivity increases and brings more carriers to centers of non-radiative recombination; consequently, the average lifetime drops.

In Fig. 4.10 b) by filled squares we show the calculated B values that indeed increase from ~1×10^{-11} cm^3/s in sample with x=0.034 up to 2.3×10^{-10} cm^{3}s^{-1} in sample with x=0.16. However, quantum efficiency, which can be represented by total area of time-integrated PL spectra, peaks around at x=0.10 and then rapidly drops for higher x. This result clearly shows that the third term in Eq. 5 cannot be attributed solely to radiative band-to-band recombination. There must be an additional physical mechanism of non-radiative nature, which recombination rate is proportional to free carrier density, at least above a specific density value. It is worth to note that within the entire excitation range no impact of C term has been observed in modeling carrier dynamics. We found out that up to 1 mJ/cm^2 (ΔN~10^{20} cm^{-3}) Auger coefficient as high as 1×10^{-30} cm^{6}s^{-1} does not have any noticeable impact on LITG decay kinetics.

Chapter 5. Excess carrier dynamics in GaAsBi layers with different Bi content

5.1 Comparison of room temperature carrier dynamics in GaAs and GaAsBi

This section is focused on comparison of carrier dynamics in GaAs and GaBiAs epitaxial layers. The investigated ~1.5 μm-thick GaAsBi layers were grown by MBE technique on semi-insulating (SI) GaAs substrates at Center for Physical Sciences and Technology (Vilnius). Different Bi content in the samples was achieved by varying growth temperature. The reference GaAs samples (8 μm-thick high quality GaAs epilayer and 300 μm-thick SI GaAs substrate) were investigated to elucidate the role of Bi alloying. Energy bandgap of the GaAsBi alloys was determined from optical absorption spectra and provided the Bi content according to E_g(Bi) dependence [15]. The dynamic grating on the samples was written using 25 ps pulses at 532 nm of YAG:Nd^{+3} laser. The grating decay was probed by a delayed probe beam at 1064 nm.

An increasing carrier recombination rate with Bi content was found at room temperature by measuring grating decay time at large grating period (Fig. 5.1). Diffraction efficiency kinetic of the GaAsBi sample with the lowest Bi content exhibited

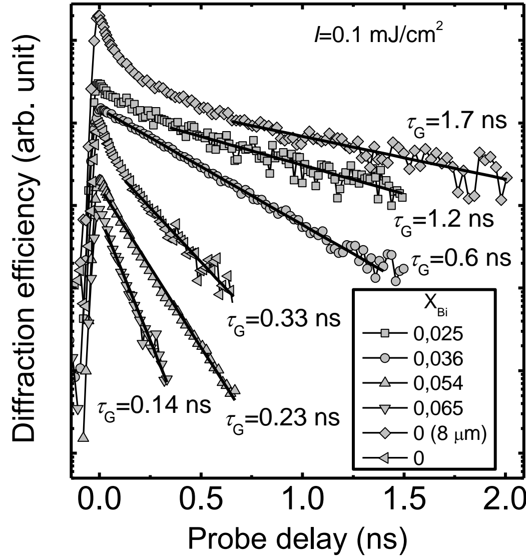

Figure 5.1. Comparison of diffraction efficiency kinetics in GaAs and GaAsBi at constant excitation fluence.

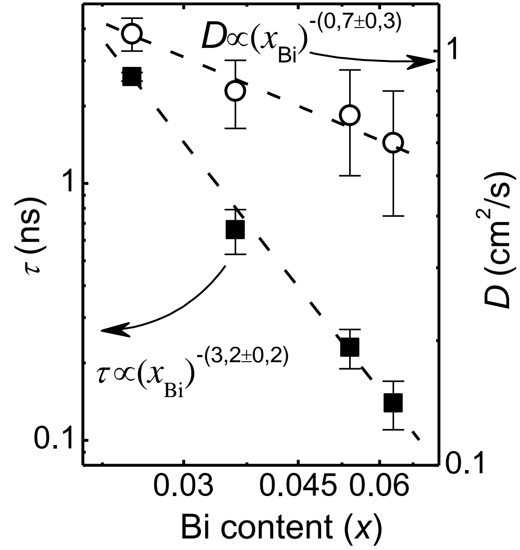

Figure 5.2. Room temperature dependence of carrier lifetime (filled squares) and diffusion coefficient (open circles) on Bi content.

nonexponential decay similar to that of GaAs. Subsequent numerical modeling of η kinetics provided carrier lifetime τ_R=2.6 ns and surface recombination velocity $S=7\times10^4$ cm/s values for the GaAsBi layer and confirmed the typical value of $S=5\times10^5$ cm/s for GaAs epilayer. The contribution of surface recombination to the grating decay was not observed in the GaAsBi samples with higher Bi content due to decreasing diffusivity and increasing carrier recombination rate in the bulk. LITG kinetics were measured for several periods of transient grating, which allowed determination of carrier lifetime τ and diffusivity D (Fig. 5.2). The fast carrier lifetime decrease with increase in Bi content revealed that incorporation of Bi increases a structural disorder in the alloys [16, 17] thus creating higher density of nonradiative recombination centers. At the interband excitation, a diffusivity of the bipolar electron-hole plasma is described by the ambipolar carrier diffusion coefficient D_a according to relationship $1/D_a=(1/D_n+1/D_h)/2$, where D_n and D_h denote the diffusion coefficients for electrons and holes. As $\mu_e>>\mu_h$ for GaAs, the condition $D_n>>D_h$ holds and leads to $D_a\approx 2D_h$. We assumed that the condition $\mu_e>>\mu_h$ was valid for GaAsBi alloys as well, because the electron mobility has been found only slightly decreasing at Bi alloying [18]. Consequently, the hole mobility $\mu_h=D_a/(2kT/e)=16$ cm^2/(V·s) was determined for $GaAs_{0.964}Bi_{0.036}$ from the measured D_a value. The determined decrease in room

temperature diffusivity at higher Bi content was ascribed to the increasing localization of nonequilibrium holes, as described in section 5.2.

5.2 Investigation of carrier lifetime and nonequilibrium hole diffusivity temperature dependences by using LITG technique

A deeper insight into mechanisms determining the D_a and τ parameters of GaAsBi alloys was reached from the study of their temperature dependences. The data (Fig. 5.3) pointed out to an inverse correlation between these parameters: the decrease of D_a at lower T was followed by the increase of τ. Saturation of low D_a value (varying with Bi content) for T<100 K and its ~10-fold increase at higher temperatures indicated that carrier mobility was thermally activated (correspondingly, ten-fold increase of τ was found at T<100 K). Numerical fit of the measured curves (Fig. 5.3) provided the thermal activation energy of diffusivity ΔE_a=46±6 meV. The reason of this effect we attributed to a strong localization of nonequilibrium holes by potential fluctuations due to Bi-related bound states [19, 20]. As the obtained ΔE_a values were approximately the same for all

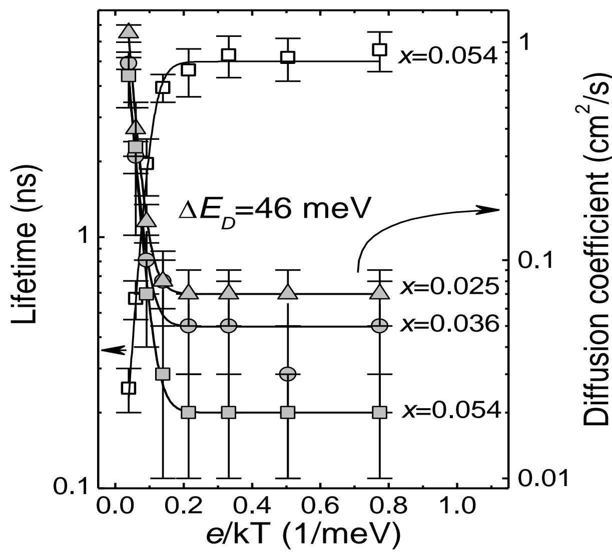

Figure 5.3. Temperature dependences of carrier lifetime (open squares) and bipolar diffusion coefficient (filled symbols) for the $GaAs_{1-x}Bi_x$ samples at excitation fluence of 30 μJ/cm^2. Solid lines represents numerical fits using Arhenius equation.

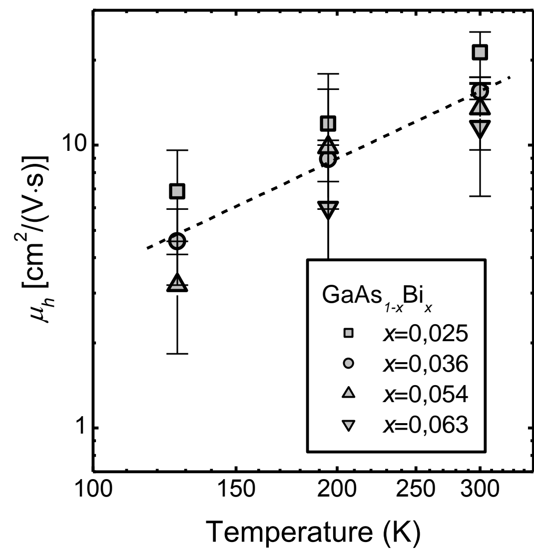

Figure 5.4. Temperature dependences of hole mobility for $GaAs_{1-x}Bi_x$ samples at excitation fluence of 30 μJ/cm^2. Dashed line is guide to an eye.

layers studied and room temperature diffusivity decreased with increase of Bi content, we assumed that the increase of Bi leads to higher density of the barriers but doesn't change the barrier height (for the range of investigated Bi concentration). The ΔE_a value being approximately twice higher than the kT at 300 K indicated that the nonequilibrium hole transport is strongly affected by localization even at room temperature. This was clearly seen from the temperature dependence of hole mobility in 100–300 K range (Fig. 5.4), which increased with temperature and did not saturate even at room temperature (similarly to the temperature dependence of the band Hall mobility in LT GaAs with extremely high point defect concentration [21]). We also note that the highest hole mobility value at room temperature (μ_h=20 cm^2/(V·s)) was by order of magnitude lower than that of GaAs (μ_h=420 cm^2/(V·s)) thus clearly demonstrating the detrimental Bi effect to mobility of nonequilibrium holes.

Conclusions of the thesis

1. The kinetics of induced bleaching reveals dynamics of the population of excited states at the probe quanta energy and doesn't allow determination of excess carrier lifetime.
2. Differential transmission technique allows determination of excess carrier lifetime by monitoring light induced free carrier absorption decay. Probe beam quanta energy needs to be ~100 meV smaller than InN energy bandgap to realize conditions for detection of free carrier absorption, not affected by induced bleaching effect.
3. Carrier recombination rate in MBE-grown InN is proportional to excess carrier density in the range 10^{18}–10^{20} cm^{-3} ($1/\tau = B^*(\Delta N + n_0)$). Numerically determined nonlinear recombination coefficient B^* value depends on background carrier density n_0 and varies from 4×10^{-10} cm^3/s in the sample with n_0=1.4×10^{18} cm^{-3} to 32×10^{-10} cm^3/s in the sample with n_0=4.7×10^{18} cm^{-3}. The nonlinear excess carrier recombination was attributed to trap-assisted Auger recombination with coefficient C_{TAAR}=B^*/N_T=$(4.5\pm2)\times10^{-28}$ cm^6/s at room temperature.
4. The density of fast nonradiative recombination centers increases with Ga content in $In_xGa_{1-x}N$ alloys with x>0.7. Latter assumption supports more efficient creation of thermal grating in the $In_xGa_{1-x}N$ layer with higher Ga content, thus pointing out what the main reason of lattice heating is not the pump photon excess energy, but the rate of nonradiative recombination, being the fastest in the $In_{0.7}Ga_{0.3}N$. Decreasing excess carrier recombination rate with temperature (295–10K) and carrier density can be explained by carrier localization in InGaN caused by (i) potential fluctuations due to inhomogeneous distribution of In or Ga atoms and subsequent carrier separation from nonradiative recombination centers; ii) presence of potential barriers around charged dislocations. The determined activation energy value ΔE of carrier recombination rate is equal to 19±1 meV.
5. An inverse correlation between increasing with temperature excess carrier lifetime ($\tau \propto T^{1/2}$) and decreasing bipolar diffusion coefficient ($D \propto T^{-1/2}$) points out that diffusion flow to extended defects (dislocations at grain boundaries) determines the carrier lifetime in a single InGaN layer. Radiative carrier

recombination with coefficient $B_{T=300K}$=7×10^{-11} cm^3/s determines the increase of carrier recombination rate with decreasing temperature (295 K>T>100 K) and increasing excess carrier density (ΔN=10^{18}–10^{20} cm^{-3}).

6. The correlation between excess carrier diffusivity and recombination rate in MOCVD-grown InGaN/GaN MQW is governed by carrier localization. The excess carrier recombination rate at high photo-excited carrier density is influenced by increase of both nonradiative and radiative recombination rates.
7. Thermal activation of carrier recombination rate and diffusivity in $GaAs_{1-x}Bi_x$ ternary alloys indicates that Bi induces potential fluctuations of energy bandgap which can localize excess carriers. The decreasing value of carrier diffusion coefficient at room temperature with Bi content and similar thermal activation energy (ΔE_D=46±6 meV) of diffusivity for all layers indicates, that Bi leads to higher density of the barriers but does not change the barrier height (for the range of investigated Bi content 0.063>x>0.025).
8. The tenfold decrease in nonequilibrium hole mobility (down to 10–20 cm^2/(V·s)), comparing to GaAs, is governed by Bi-induced potential fluctuations in the MBE-grown $GaAs_{1-x}Bi_x$ (0.063>x>0.025) layers.

References

1. F. Chen, A. N. Cartwright, H. Lu, and W. J. Schaff, Journal of Crystal Growth, **269**, 10 (2004).

2. V. Pacebutas, G. Aleksejenko, A. Krotkus, J. W. Ager, W. Walukiewicz, H. Lu, and W. J. Schaff, Applied Physics Letters, **88**, 191109 (2006).

3. F. Chen, A. N. Cartwright, H. Lu, and W. J. Schaff, Applied Physics Letters, **83**, 4984 (2003).

4. B. Arnaudov, T. Paskova, P. P. Paskov, B. Magnusson, E. Valcheva, B. Monemar, H. Lu, W. J. Schaff, H. Amano, and I. Akasaki, Physical Review B, **69**, 115216 (2004).

5. A. Dmitriev and A. Oruzheinikov, Journal of Applied Physics, **86**, 3241 (1999).

6. A. Mohanta, D. J. Jang, G. T. Lin, Y. T. Lin, and L. W. Tu, Journal of Applied Physics, **110**, 023703 (2011).

7. S. P. Fu, Y. F. Chen, and K. Tan, Solid State Communications, **137**, 203 (2006).

8. H.-C. Wang, Y.-C. Lu, C.-C. Teng, Y.-S. Chen, C. C. Yang, K.-J. Ma, C.-C. Pan, and J.-I. Chyi, Journal of Applied Physics, **97**, 033704 (2005).

9. S. Chichibu and T. Azuhata, Applied Physics Letters, **70**, 2822 (1997).

10. J. L. Farvacque, Z. Bougrioua, and I. Moerman, Physical Review B, **63**, 115202 (2001).

11. T. Malinauskas, K. Jarasiunas, M. Heuken, F. Scholz, and P. Brückner, Physica Status Solidi C, **6**, S743 (2009).

12. R. Aleksiejunas, M. Sudzius, T. Malinauskas, J. Vaitkus, K. Jarasiunas, and S. Sakai, Applied Physics Letters, **83**, 1157 (2003).

13. P. Scajev, K. Jarasiunas, S. Okur, U. Ozgur, and H. Morkoc, Journal of Applied Physics, **111**, 023702 (2012).

14. P. Scajev, A. Usikov, V. Soukhoveev, R. Aleksiejunas, and K. Jarasiunas, Applied Physics Letters, **98**, 202105 (2011).

15. K. Alberi, O. D. Dubon, W. Walukiewicz, K. M. Yu, K. Bertulis, and A. Krotkus, Applied Physics Letters, **91**, 051909 (2007).

16. M. Henini, J. Ibanez, M. Schmidbauer, M. Shafi, S. V. Novikov, L. Turyanska, S. I. Molina, D. L. Sales, M. F. Chisholm, and J. Misiewicz, Applied Physics Letters, **91**, 251909 (2007).

17. S. Tixier, M. Adamcyk, T. Tiedje, S. Francoeur, A. Mascarenhas, P. Wei, and F. Schiettekatte, Applied Physics Letters, **82**, 2245 (2003).

18. R. N. Kini, L. Bhusal, A. J. Ptak, R. France, and A. Mascarenhas, Journal of Applied Physics, **106**, 043705 (2009).

19. R. A. Faulkner, Physical Review, **175**, 991 (1968).

20. J. J. Hopfield, D. G. Thomas, and R. T. Lynch, Physical Review Letters, **17**, 312 (1966).

21. J. Betko, M. Morvic, J. Novak, A. Forster, and P. Kordos, Applied Physics Letters, **69**, 2563 (1996).

List of publications related to the thesis

Papers:

P1. **S. Nargelas**, T. Malinauskas, K. Jarašiūnas, E. Dimakis, A. Georgakilas, „Investigation of optical nonlinearities and carrier dynamics in In–rich InGaN alloys“, Acta Physica Polonica A, **113**, 839–843 (2008).

P2. **S. Nargelas**, T. Malinauskas, A. Kadys, E. Dimakis, T.D. Moustakas, K. Jarašiūnas, „Nonlinear carrier recombination and transport features in highly excited InN layer“, Phys. Stat. Solidi C, **6**, S735–S738 (2009).

P3. **S. Nargelas**, R. Aleksiejūnas, K. Jarašiūnas, M. Vengris, „Light induced bleaching and absorption kinetics in highly excited InN layers“, Phys. Stat. Solidi C, **6**, 2632–2634 (2009).

P4. **S. Nargelas**, R. Aleksiejūnas, M. Vengris, T. Malinauskas, K. Jarašiūnas, E. Dimakis, „Dynamics of free carrier aborption in InN layers“, Apl. Phys. Lett., **95**, 162103 (2009).

P5. **S. Nargelas**, R. Aleksiejūnas, M. Vengris, K. Jarašiūnas, „Carrier relaxation Dynamics in InN investigated by femtosecond pump-probe technique“, Phys. Stat. Solidi C, **7**, 1853–1855 (2010).

P6. **S. Nargelas**, K. Jarašiūnas, K. Bertulis, V. Pačebutas, „Hole diffusivity in GaAsBi alloys measured by picosecond transient grating technique“, Apl. Phys. Lett., **98**, 082115 (2011).

P7. T. Malinauskas, A. Kadys, T. Grinys, **S. Nargelas**, R. Aleksiejūnas, S. Miasojedovas, J. Mickevičius, R. Tomašiūnas, K. Jarašiūnas, M. Vengris, S. Okur, V. Avrutin, X. Li, F. Zhang, U. Ozgur, H. Morkoc, „Impact of carrier localization, recombination, and diffusivity on excited state dynamics in InGaN/GaN Quantum wells“, Gallium Nitride Materials and Devices VII, Proc. of SPIEE, **8262**, 82621S (2012).

P8. K. Jarašiūnas, R. Aleksiejūnas, T. Malinauskas, **S. Nargelas**, P. Ščajev, „Nonlinear optical technicues for characterization of wide bandgap semiconductor electronic properties: III–nitrides, SiC and diamonds“, MRS Proceedings, **1396**, 147–158 (2012).

Conference contributions

K.1 **S. Nargelas**, T. Malinauskas, K. Jarasiunas, E. Dimakis, and A. Georgakilas, „*Investigation of optical nonlinearities and carrier dynamics in In-rich InGaN alloys*“, International Symposium on Ultrafast Phenomena in Semiconductors (UFPS-13), August 26–29, 2007, Vilnius, Lithuania. (oral presentation)

K.2 **S. Nargelas**, T. Malinauskas, A. Kadys, E. Dimakis, T.D. Moustakas, and K. Jarasiunas, "*Nonlinear carrier recombination and transport features in highly excited InN layer*", International Workshop on Nitride Semiconductors (IWN2008), October 6–10, 2008, Montreux, Switzerland. (oral presentation)

K.3 **S. Nargelas**, T. Malinauskas, A. Kadys, K. Jarašiūnas, M. Vengris, E. Dimakis, T.D. Moustakas, "*Investigation of optical nonlinearities in InN layers by using time-resolved differential transmission and light-induced transient grating techniques*", European Materials Research Society (E-MRS) Fall Meeting, September 14–18, Warsaw, Poland. (poster presentation)

K.4 **S. Nargelas**, R. Aleksiejūnas, M. Vengris, K. Jarašiūnas, „*Carrier recombination in InN investigated by femtosecond pump-probe technique*“, 8th International Concefernce on Nitride Semiconductors (ICNS-8), October 18–23, 2009, Jeju Island, Republic of Korea. (poster presentation)

K.5 **S. Nargelas**, R. Aleksiejūnas, K. Jarašiūnas, M. Vengris, "*Nonlinear carrier recombination in highly excited InN layers*", 15th Semiconducting and Insulating Materials Conference (SIMC-XV), June 15–19, 2009, Vilnius, Lithuania. (poster presentation)

K.6 K. Jarašiūnas, T. Malinauskas, R. Aleksiejūnas, A. Kadys, **S. Nargelas**, V. Gudelis, „*Innovative Time-Resolved Optical Characterization Techniques for Monitoring of Carrier Dynamics in Wide Band Gap Semiconductors*“, 52nd Electronic Materials Conference, June 23–25, 2010, Notre Dame, Indiana, USA. (oral presentation)

K.7 **S. Nargelas**, K. Jarasiunas, V. Pačebutas, „*Optical diagnostics of GaBiAs/GaAs heterostructures with varying Bi content*“, 10th Expert Evaluation & Control of Compound Semiconductor Materials & Technologies, May 19–21, 2010, Darmstadt, Germany. (oral presentation)

K.8 T. Malinauskas, A. Kadys, T. Grinys, **S. Nargelas**, S. Miasojedovas, K. Jarašiūnas, J. Mickevičius, R. Tomašiūnas, „*Optical studies of carrier dynamics in InGaN/GaN MQWs with different In content*“, 9th International

Concefernce on Nitride Semiconductors (ICNS-9), July 10–15, Glasgow, Scotland. (poster presentation)

K.9 T. Malinauskas, A. Kadys, T. Grinys, **S. Nargelas**, S. Miasojedovas, K. Jarašiūnas, J. Mickevičius, R. Tomašiūnas, „*Recombination and diffusion of carriers in strained InGaN/GaN MQWs with different In content*“, Advanced Optical Materials and Devices (AOMD-7), August 28–31, 2011, Vilnius, Lithuania. (oral presentation)

K.10 T. Malinauskas, A. Kadys, T. Grinys, **S. Nargelas**, S. Miasojedovas, K. Jarašiūnas, J. Mickevičius, R. Tomašiūnas, „*Poliarizacinių laukų ir lokalizacijos įtaka nepusiausvirųjų krūvininkų dinamikai InGaN/GaN kvantiniuose lakštuose su skirtingu In kiekiu*“, 39–oji Lietuvos nacionalinė fizikos konferencija, Spalio 6–8 d., Vilnius, Lietuva. (oral presentation)

K.11 **S. Nargelas**, A. Kadys, K. Jarašiūnas, K. Bertulis, V. Pačebutas, E. Dimakis, T. Malinauskas, „*Investigation of carrier recombination and diffusion in III generation photovoltaic materials*”, Next Generation Solar Energy From Fundamentals to Applications, December 12–14, 2011, Erlangen, Germany. (poster presentation)

K.12 K. Jarašiūnas, R. Aleksiejūnas, **S. Nargelas**, T Malinauskas, S. Miasojedovas, A. Kadys, S. Okur, X. Li, Ü. Özgür, H. Morkoç, O. Tuna, M. Heuken, „*On injection-activated defect recombination in InGaN layers*”, 9th International Symposium on Semiconductor Light Emitting Devices, July 22–27, 2012, Berlin, Germany. (oral presentation)

K.13 R. Aleksiejūnas, P. Ščajev, **S. Nargelas**, T. Malinauskas, A. Kadys, K. Jarašiūnas, „*Impact of diffusivity to carrier recombination ratein nitride semiconductors: from bulk GaN to(In,Ga)N quantum wells*“, International Workshop on Nitride Semiconductors 2012, 14–19 October, 2012, Sapporo, Japan. (oral presentation)

K.14 **S. Nargelas**, K. Jarašiūnas, M. Vengris, T. Yamaguchi, Y. Nanishi, “*Injection-activated defect-governed recombination rate in InN*“, International Workshop on Nitride Semiconductors 2012, 14–19 October, 2012, Sapporo, Japan. (poster presentation)

Information about the author

Name and surname:	Saulius Nargelas	
Birth date and place:	March 5, 1984, Utena, Lithuania	
E-mail:	saulius.nargelas@ff.vu.lt	
Education:	2002	Secondary education, Utena „Saulės“ gymnasium
	2006	Bachelor degree in Physics, Vilnius University
	2008	Master degree in Physics, Vilnius University
	2008–2012	Doctoral studies at Vilnius University
Scientific experience:	2005–2006	Technician at the Institute of Materials Science and Applied Research, Vilnius University (part-time)
	2006–2011	Engineer at the Institute of Applied Research, Vilnius University (part-time)
	2011–till now	Junior scientific researcher at the Institute of Applied Research, Vilnius University (part-time)
Specialization:		Optical characterization of semiconductors by using light-induced transient gratings and differential transmission techniques, numerical modeling of carrier dynamics.
Publications:		Co-author of 14 papers listed in Thomson Reuters ISI WOS^{SM}.